Elastic reinforcement and yielding of starch-filled lipid gels

Braulio A. Macias-Rodriguez[a,b*], *Krassimir P. Velikov*[a, b, c*]

[a] Unilever Innovation Centre Wageningen, Bronland 14, 6708 WH Wageningen, the Netherlands.

[b] Institute of Physics, University of Amsterdam, Science Park 904, 1098 XH Amsterdam, The Netherlands.

[c] Soft Condensed Matter, Debye Institute for Nanomaterials Science, Utrecht University, Princetonplein 5, 3584 CC Utrecht, The Netherlands.

ABSTRACT

Many foods involve complex suspensions of assorted particles in a Newtonian liquid or viscoelastic solid continuous medium. In this work, we study the case of suspensions of non-Brownian non-interacting rigid particles: starch, embedded in a soft solid: a colloidal lipid gel. We relate the macroscopic properties of the suspensions to the mechanics of the colloidal gel and the particle volume fraction. As particle volume fraction increases, the suspension gradually stiffens and becomes brittle as the system approaches its maximum packing fraction, the latter determined empirically by a Krieger-Dougherty type law. The elastic modulus, yield stress and yield strain are interrelated through simple scaling laws from micromechanical homogenization analysis of hard

spheres isotropically-distributed in yield stress fluids. These laws enable estimation of nonlinear properties from linear properties at modest and finite deformations.

1. INTRODUCTION

Structured foods often comprise particulate fillers dispersed in a continuous matrix. For example, confectionery and savory foods, and plant-based meats include suspensions of hydrophilic particles: sugar, salt or texturized protein grains, and hydrophobic cocoa particles, dispersed in a hydrophobic lipid, or a hydrophilic protein phases or mixtures thereof. The nature of the filler, e.g. size, rigidity and surface texture, and particle physical interactions, e.g. filler-filler or filler-matrix interactions, have profound effects on mechanical properties (Wijmans and Dickinson 1998; Heinrich et al., 2002; Genovese 2012). Added to this intricacy, the physical properties of the fillers rarely exist at equilibrium but evolve during processing.

A first step towards in understanding the mechanisms underlying reinforcement and flow of particulate foods consists in applying knowledge from wet granular suspensions and elastic reinforcement physics to simplified model food recipes (Heinrich et al., 2002; Mitarai and Noris 2006; Behringer and Chakraborty 2018). A plethora of studies on suspensions and particle-filled composites have been reported in the literature (Scholten 2017). Herein, we review salient research efforts compositionally relevant to our model system.

Similar to suspensions of granular hard spheres, the relative high-shear shear-thickened viscosity η_2/η_0 or η_r of dense 'chocolate' crumbs (a dried mixture of sucrose crystals, milk, and cocoa mass) obeys: $\eta_r = A\left(1-\frac{\phi}{\phi_J^{\mu}(\sigma)}\right)^{-\lambda}$, where η_0 is the viscosity of the continuous phase, and $A \simeq 1$, and $\lambda \simeq 2$ for spheres (Blanco et al., 2019). The jamming point ϕ_J is a function of both the interparticle friction coefficient μ, with values $\mu \to 0$ for 'smooth' and $\mu \gtrsim 1$ for 'rough' particles, and the applied stress σ which triggers particle contact jamming when it exceeds a critical σ^*. By measuring viscosity of

crumbs undergoing processing at increasing ϕ, a state diagram revealed that conching and lecithin addition maximize the flowable solid content before jamming occurs, by changing the state of aggregation of the particles and tuning their interparticle friction and adhesion.

This framework has been extended to provide a geometric definition of jamming ϕ_J, based on the theoretical hard sphere basis for the random close packing fraction as a function of particle size distribution (Shewan et al., 2021). The model has been applied to interpret the rheological behavior of sugar-fat particles suspended in a molten lipid phase (Shewan et al., 2021). A modified Maron-Pierce-Quemada (MPQ) model has been proposed: $\eta_r = \left(1 - \frac{\phi}{\phi_{\mathrm{rcp}}}\right)^{-2}$, which is a linearized form where the intercept with x-axis is equal to ϕ_{rcp} of non-attractive hard and soft sphere suspensions. The maximum packing fraction deviates from its theoretical values when attractive interactions exist and the percolation threshold is reached, i.e. $\phi_m < \phi_{rcp}$, that leads to an filler volume-spanning network. The elasticity of such network is modelled according to percolation theory as: $G' = \beta(\phi - \phi_m)^{\alpha}$ where ϕ_m is obtained from the experimental viscosity data, considering size distribution effects, and α and β are parameters derived from free fitting.

Another paradigm that has successfully described the effect of adding fractal-like silica fillers on cross-linked gels and rubbers has been recently proposed. The significance of this model lies on the incorporation of filler-size dependence on the elasticity of composite systems, often neglected in classical continuum models which are scale free (Mermet-Guyennet et al., 2017). The linear viscoelastic reinforcement R_{LVE} of the composite follows:

$R_{LVE} \equiv \frac{G'(\phi)}{G'(\phi=0)} - 1 = 2.5\phi + \delta \frac{G_f'}{G_m'} \frac{\phi^3}{r}$, where R_{LVE} is defined as the ratio of the storage modulus of the filled material to that of the matrix less 1, the subscripts *f* and *m* refer to the filler and matrix

material, r is the effective radius of the filler and δ is a dimensional coefficient attributed to a characteristic length-scale (Mermet-Guyennet et al., 2017).

In our study, we investigate the reinforcement effect of hydrophilic starch particles dispersed in a hydrophobic soft viscoelastic lipid (crystals dispersed in oil) continuous phase. Hence, it represents a progression from past studies focused on concentrated suspensions dispersed in liquid oil continuous medium (Zhou et al., 1995; Blanco et al., 2019; Richards et al., 2020; Shewan et al., 2021). We use a chemically modified starch as it is a ubiquitous filler in food suspensions and serves as a good model material due to its limited swelling and gelatinization in non-aqueous solvent, so that phase volume corrections are avoided. In addition, starch lacks physical interactions with the lipid viscoelastic matrix, so it can be deemed as a passive filler. Despite the seemingly complex nature of our model system, we model the flow behavior according to a micromechanical analysis for hard monodisperse spheres suspended in yield-stress fluids. Remarkably, the full mechanical response at linear and nonlinear modest and fine shear strains, can be predicted using simple scaling arguments based on particle volume fraction and maximum packing fraction. Our findings are relevant to food processing and sensory perception of dense food-based suspensions (concentrates), where filler addition is often sought to modulate stiffness, and processability of composite materials.

2. MATERIALS AND METHODS

2.1.Materials

Soybean oil and glyceryl tripalmitate (≥85%) were obtained from Sigma-Aldrich (Netherlands). Thermflo starch was obtained from Ingredion (UK). Thermflo® starch is a chemically modified maize starch with high tolerance to heat and shear. The mass and quoted densities of the materials: 0.92 g/cm^3 at 25 °C (soybean oil), 0.8901 g/cm^3 at 47 °C (supercooled tripalmitin) and 1.5 g/cm^3

(starch) were used to calculate volume fractions. [19] For starch particles, their mass, having ~11 % native moisture content, was taken into consideration when estimating volume fractions. Since the starch particles do not dissolve nor swell in oil, we assume that the volume fraction remain constant in this solvent. Estimation of volume fractions introduces an error in the vicinity of ~5–10% even for a highly monodisperse hard spheres (Poon et al., 2012).

2.2.Sample preparation

Lipid mixtures at fixed glyceryl tripalmitate volume fraction ϕ = 0.1 were heated and hold at 70 °C for 10 min, well above the triglyceride melting temperature, 54 °C. Starch was added at increasing ϕ = 0.1-0.5 to the melt and hold for an additional 5 min while stirring at 1000 min^{-1} to ensure thermal equilibration and homogeneity of the samples. Suspensions were rapidly cooled and held at 5 ºC for approximately 120 min to promote small crystal formation, and then brought to 20 ºC for crystal aggregation to ensue. Samples were manually stirred to maximize isotropic distribution of particles in the continuous medium and to avoid incorporation of air in the gel resultant from vigorous mechanical mixing. Measurements were performed after a week to allow any remnant crystallization to culminate.

2.3.Microscopy

Scanning electron microscopy (SEM)

High resolution SEM were conducted on a with Scanning Electron Microscopy (TM Hitachi 3000). The sample was sputtercoated with platinum (120 s) for a better SEM contrast and to prevent charging by the electron beam.

2.4.Transmitted light microscopy

Samples were carefully sandwiched between glass slides and cover slips and were visualized using via light microscopy (MOR2410, Malvern, United Kingdom) with a 5× magnification objective.

The microscopy was operated in bright-field and polarized modes. Samples were prepared on glass slides at similar melting and crystallization detailed in the Sample Preparation section.

2.5.Confocal microscopy

Samples were visualized with a confocal laser scanning microscope (CLSM) (Zeiss, Oberkochen, German) with 20× and 40× magnification objectives. A fluorescent dye Nile Red was used to label the continuous oil phase. Oil was detected using a laser with 488 nm excitation wavelength respectively. Intensity data were collected at emission wavelength ranges of 600-680 nm. Images were collected at ϕ_{filler} = 0.1-0.2 since higher vol. fraction preclude image acquisition due to multiple scattering and wall effects. Micrographic 'tiles' of 25 pictures were collected and analyzed to determine the size distribution of the non-spherical starch granules according to their Feret or "caliper" diameter, defined as the longest distance between two parallel planes restricting the object perpendicular to that direction. Micrographs tiles were processed in Fiji Image J (Version 1.52p) by applying an automatic threshold and watershed plugin. Particle counting was determined using the analyze particle plugin, discarding particles in the edges (Refer to Supporting Information for example and higher magnification images).

2.6.Shear rheology

Rheological properties were determined using a torque-controlled rheometer (MCR 302, Anton Paar GmbH, Germany) equipped with parallel-plate serrated geometries DIA: 25 mm to circumvent wall slip. In order to perform measurements of thixotropic materials, namely lipid gels, with a reproducible initial state, samples were manually stirred during their preparation and rested for 10 min post loading to allow relaxation of internal stresses. This procedure was adopted to avoid shear-induced migration of particles, inadvertently introduced by preshear protocols, and to

promote isotropic distribution of particles. Measurements were conducted at a fixed gap height of h = 1 mm, much larger than the particle granular size observed microscopically. After fixing the gap, the following procedure was applied: i) oscillations are applied within the linear regime γ_0 = 0.01 % and ω = 2 rad/s for t = 5 min to obtain the plateau elastic modulus G'; ii) a subsequent amplitude sweep $\gamma_0 = 10^{-3}$-10^{3} % at the same frequency or small rotational velocity are imposed to obtain the yield stress σ_y. The initial elasticity measurement is nonperturbative as the same yield stress is measured with or without linear pre-oscillations. The two approaches to measure dynamic yield stresses are utilized for comparative purposes, and since it was not known a priori whether oscillatory shear would induce anisotropic structures to larger degree due to the application of multiple oscillatory cycles at each shear strain input, compared to a rotational shear. Irrespective of the measuring method, yield stress occurs when stress is maximal: $\sigma(R) = \frac{T}{2\pi HR^2}$ for a parallel plate of arbitrary R radius. Yield stress were estimated at the 'flow point' $G' = G''$ and intersection of stress growth curves, and can be deemed as the total stress that triggers full flow of the pastes. The yield strain was empirically estimated as the point at which the linear elastic modulus decreases to 90% of its initial value. Although arbitrary, this procedure was able to capture experimentally the effect of the filler on triggering flow. Approaches such as determining the yield strain from 'line intersections' of the elastic modulus, yield strain at the flow point $G' = G''$ or stress-growth experiments were unsuccessful, as either the strain varied very little or it was ill-defined. Some of the advantages and disadvantages of using these methods to determine the yield stress and strain have been recently reviewed (Dinkgreve et al., 2016). Elastic moduli and yield stresses of the pastes as a function of volume fraction of embedded particles were measured. It is noteworthy that high ϕ, non-uniform distribution of stress and strain throughout the material is

more likely to occur. Estimation of rheological measurements introduces an error in the range of ±5–10%.

3. RESULTS AND DISCUSSIONS

Fig. 1 shows a representative sample of the composite system, the starch-filled gel. Starch particles had an irregular shape and an average size of ~ 10 μm present as individual granules or agglomerates (Fig. 1a), whereas the lipid gel network is a colloidal in network with aggregates as large as ~50 μm (See Supporting Information for higher magnification micrographs). Both, starch dispersed in oil or lipid phases and subject to similar thermal/crystallization regimes similar to the suspensions share similar morphology (Fig. 1b and 1c). Starch dispersed in the continuous colloidal gel also appears to display more clustering due to growth of lipid crystals aggregates occupying free volume. Birefringence is also present hinting that starch particles maintain their integrity post thermal treatment due to the crosslinking nature of starch and absence of water, which supports the notion that changes in phase volume of starch with and without thermal treatment are negligible.

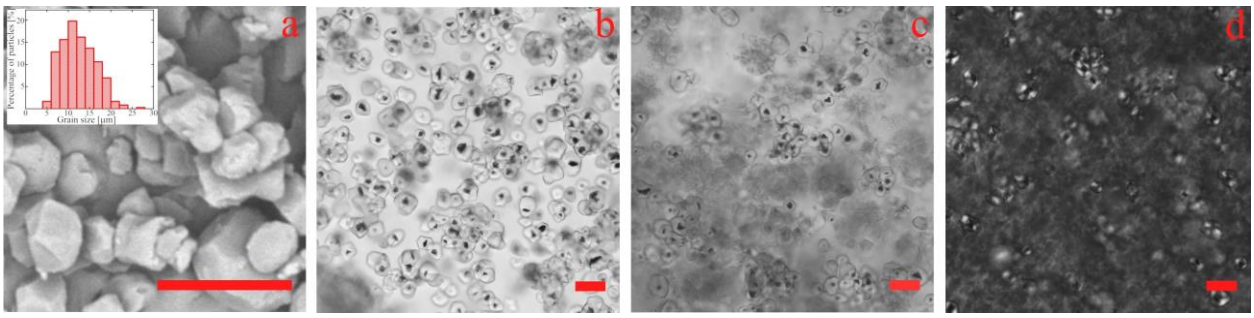

Figure 1. SEM micrograph of the Thermoflo® starch (a) and their corresponding grain size distribution (inset). Micrographs of starch in oil (b) and starch in lipid gel $\phi_{\text{tripalmitin}} = 0.1$ (c) at constant volume fraction $\phi_{\text{starch}} = 0.1$. Lipid crystal aggregates appear as floc-like aggregates. Polarized micrograph (d) of (c). Sample (b), (c), (d) were subjected to similar melting/crystallization protocols. Scale bar in all figures equal 25 μm.

Fig. 2 presents the linear viscoelastic moduli G', G'' of the lipid colloidal gel at fixed volume fraction $\phi_{\text{tripalmitin}} = 0.10$ (Fig 2a) as a function of frequency, and the time evolution of the elastic modulus of the pure paste $\phi_{\text{starch}} = 0$ compared to a sample embedded with starch particles $\phi_{\text{starch}} = 0.3$. It is observed that $G' > G''$ displays weak frequency dependence as expected for soft solids. The elastic modulus G' weakly increases over time characteristic of thixotropic materials. We infer that any increase of G' with filler volume fraction ϕ as a function of time is due to structuration of the lipid phase, and in the absence of any physical interaction between the particle and paste, the time evolution of G' of the 'continuum' remains similar. This is supported by the absolute elastic moduli and dimensionless moduli normalized by G'_0 at $\phi_{starch} = 0$ as function of time, which display similar structuring kinetics.

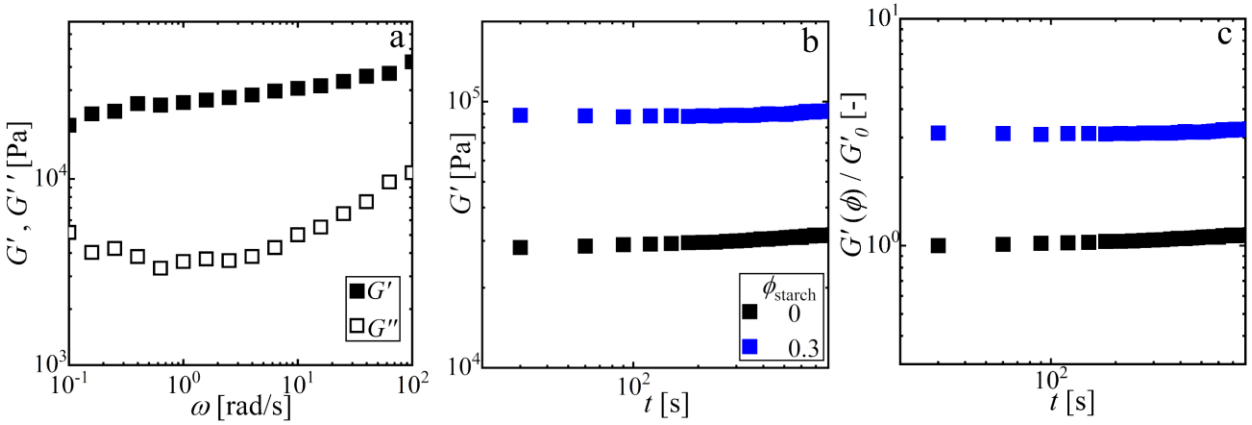

Figure 2. Frequency sweep of the lipid viscoelastic gel at fixed volume fraction $\phi_{tripalmitin} = 0.1$ (a). Absolute elastic moduli (a) and dimensionless elastic moduli $G'(\phi) / G'_0$ (b) as a function of time, for representative samples with $\phi_{starch} = 0$ and $\phi_{starch} = 0.3$.

While the evolution of the mechanical properties with ϕ are nearly frequency-independent within the linear regime, the yield stress depends on the experimental timescale and the measuring method (Dinkgreve et al., 2016). Next, we present the findings of the elastic modulus and yield stress/strain measurements as a function of starch granule volume fraction ϕ = 0-0.5. The impact of granular fillers embedded in the lipid gel on the mechanical properties, can be assessed by measurements of the linear elastic modulus G' and yield stress σ_y. Full strain amplitude oscillatory shear sweeps and stress-growth steady shear experiments at each volume fraction are included in the Supporting Information.

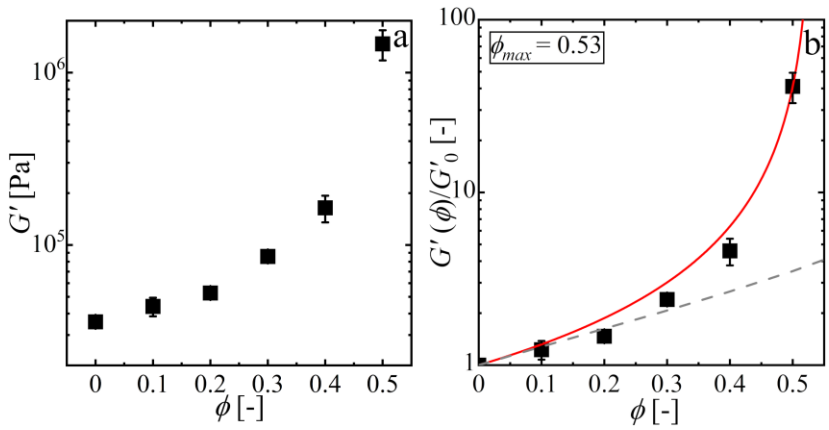

Figure 3. Absolute elastic modulus G' (a), and dimensionless elastic modulus $G^{'}(\phi) / G^{'}(0)$ (b) as function of starch volume fraction ϕ. Volume fraction of the solid lipid phase remained fixed ϕ = 0.10. The scaling of $G^{'}(\phi) / G^{'}_0$ is above the theoretical lower bound (grey dotted line) for biphasic materials with infinitely rigid inclusions (Eq. 1) and is fitted to an empirical Krieger-Dougherty type law (red line) with maximum packing fraction ϕ_m = 0.53 (Eq. 2).

We summarize these results performed on all samples with increasing volume fraction, focusing particularly on the evolution of the dimensionless modulus $G^{'}(\phi) / G^{'}(0)$ and the dimensionless yield stress $\sigma_y(\phi) / \sigma_y(0)$ to isolate the mechanical contribution of the particles to the paste. Both functions account for the mechanical strengthening of the material due to the presence of rigid inclusions. Absolute average values of the rheological measurements with their standard deviations are also presented. We note that all data points fall above a theoretical lower bound for the effective elastic moduli of quasi-isotropic and quasi-homogeneous biphasic materials given by Hashin and Shtrikman (1963):

$$\frac{G^{'}(\phi)}{G^{'}_0} > \frac{2+3\phi}{2-2\phi} \qquad (1)$$

For infinitely rigid inclusions of arbitrary geometry, namely starch $G^{'} \approx 3$ GPa, dispersed in an elastic matrix such as lipid gel $G^{'}_{0} \approx 0.03$ GPa (Schroeter and Hobelsberger 1992). In the same way, inclusion of particles at low volume fraction $\phi \leq 0.1$ shall follow a scaling $G^{'}(\phi) / G'_0 = 1 + 2.5\phi$ like Einstein's law for the effective viscosity of a dilute suspensions of noncolloidal particles. The effect of the particle concentration on the elastic modulus is significant, even for low volume fraction of inclusions, we find $G'(\phi) \approx 1.5 \times G'_0$ for $\phi = 20\%$ and $G'(\phi) \approx 24.4 \times G'_0$ for $\phi = 50\%$ as the systems approaches its maximum packing fraction. We observed that all our data can be fitted to a simple Krieger-Dougherty law:

$$\frac{G^{'}(\phi)}{G^{'}_{0}} = \frac{1}{(1-\phi/\phi_m)^{2.5\phi_m}}, \qquad (2)$$

We find that the Krieger-Dougherty law describes well the data over the examined range of volume fractions with a $\phi_m = 0.53$, obtained with a least-squares fitting method $R^2 = 0.99$, at which $G^{'}(\phi) / G^{'}_{0} \rightarrow \infty$. Expectedly, the good agreement of the model with our data supports that the elasticity of a suspension of rigid particles in a linear elastic material is analogous to the problem of the viscosity a suspension of rigid particles in a Newtonian linear fluid. The maximum packing fraction $\phi_m = 0.53$ is close to that reported for granular monodisperse spherical particles $\phi_m = 0.57$ embedded in an emulsion, Carbopol gel or bentonite suspension (Mahaut et al., 2018), but much lower than that reported for viscosity of hard-sphere suspensions $\phi_m = 0.63$ (Genovese 2002). The former inconsistency lies in the fact that in this model, ϕ_m is an empirical free-fitting parameter, sensitive to errors introduced by particle size distribution and anisotropy and mechanical determination near ϕ_J. The latter inconsistency is arguably due to shear-induced structural anisotropy inadvertently induced during viscosity measurements (Genovese 2002).

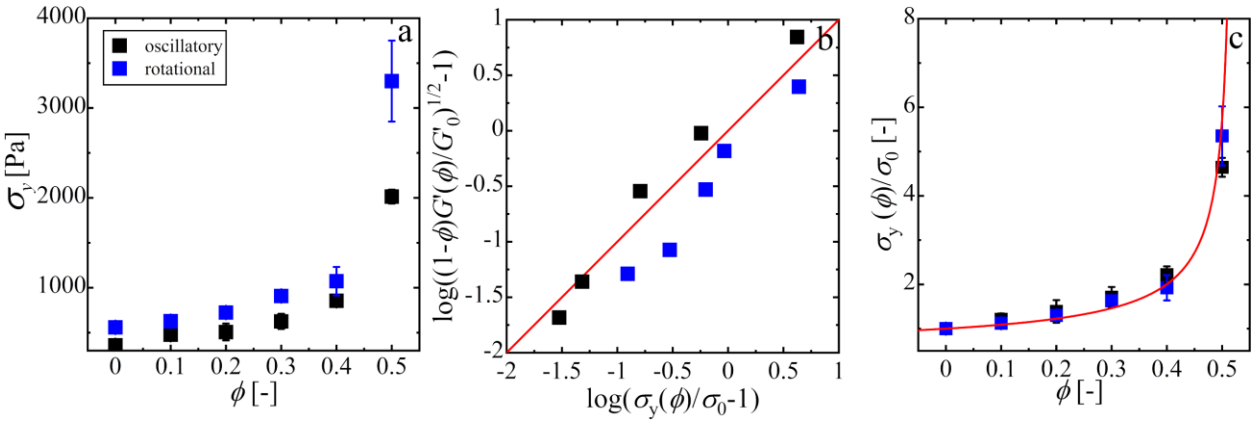

Figure 4. Absolute yield stress σ_y vs. filler volume fraction, as measured by oscillatory and rotational shear (a). Dimensionless yield stress $\sigma_y(\phi) / \sigma_0$ vs. a function of the dimensionless elastic modulus (b), described in Eq. (3) and symbolized by the red line. Dimensionless yield stress σ_y vs. filler volume fraction (c), fitted to Eq. (4) with maximum packing fraction ϕ_m = 0.53, and symbolized by the red line.

Now, we turn our attention to the yield stress of the suspensions obtained using oscillatory shear and rotational shear measurements. In Fig 4, we plot values of absolute yield stress $\sigma_y(\phi)$ and dimensionless yield stress $\sigma_y(\phi) / \sigma_0$, and observed a similar qualitative trend irrespective of measuring method: the yield stress is less sensitive to the inclusion of granular fillers to the linear elastic moduli, e.g. we find $\sigma_y(\phi) \approx 1.3 \times \sigma_0$ for $\phi = 20\%$ and $\sigma_y(\phi) \approx 5 \times \sigma_0$ for $\phi = 50\%$. Expectedly, we do find differences in the absolute values of σ_y are measurement-dependent (Dinkegreve et al., 2016).

To establish a relationship between the dimensionless elastic modulus and yield stress is challenging as the result depends on the micromechanical scheme utilized. An approach relevant to our model system is the following, discussed in (Mahaut et al., 2018):

$$\frac{\sigma_y(\phi)}{\sigma_0} = \sqrt{(1-\phi)\frac{G'(\phi)}{G_0'}} \qquad (3)$$

The micromechanical estimate of this model is based on various assumptions including: filling particles are rigid, monodisperse and noncolloidal; physical interactions between the particles and the continuous phase are absent; the distribution of the particles is isotropic. Although our particle fillers deviates from some of these geometrical postulates, e.g. non-sphericity of starch particles, it is possible to test experimentally the validity of the theoretical predictions against our model systems.

In Fig. 4b, we plot the dimensionless yield stress $\sigma_y(\phi) / \sigma_0$ as a function of the dimensionless elastic modulus $\sqrt{(1-\phi)G'(\phi)/G_0'}$ for all the systems studied in logarithmic coordinates. We observe that that there is a good agreement between our results and the micromechanical estimation of Eq. 3, that is plotted as a straight-line y = x in these coordinates. Combining Eq. 2 and Eq. 3, the yield stress equation reads:

$$\frac{\sigma_y(\phi)}{\sigma_0} = \sqrt{\frac{1-\phi}{\left(1-\phi/\phi_m\right)^{2.5\phi}}} \qquad (4)$$

With $\phi_m = 0.53$, which is plotted in Fig. 4c, and fits well the experimental data, with a least square fitting $R^2 = 0.98$.

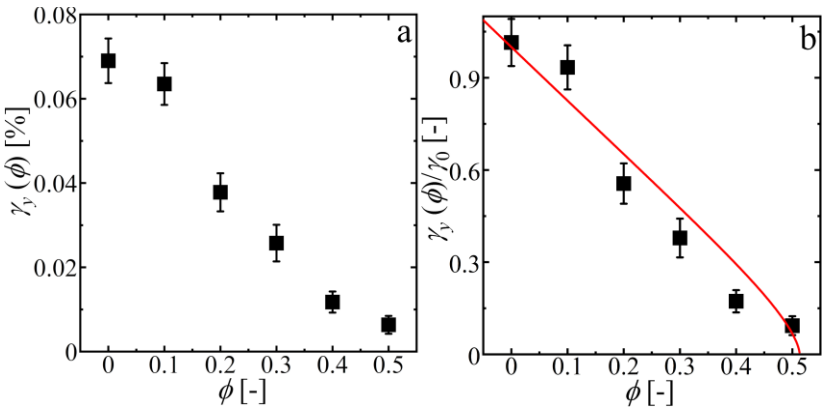

Figure 5. Absolute yield strain γ_y (a) and dimensionless yield strain $\gamma_y(\phi) / \sigma_0$ vs. filler volume fraction, as measured by oscillatory and rotational shear. Dimensionless yield strain (b) fitted to Eq. (5) with maximum packing fraction $\phi_m = 0.53$, symbolized by the red line.

In Fig 5, we plot values of the critical yield strain $\gamma_y(\phi)$ and the dimensionless yield strain $\gamma_y(\phi) / \gamma_0$. We selected this measure as we attempted unsuccessfully to determine the yield strain from various ways as noted in the Materials and Methods section Rheology. We observed that as starch volume fraction increases, the particle-filled gels becomes gradually more brittle, e.g. we find that γ_y drops almost an order of magnitude as ϕ_{starch} increases from 0% to 50%. As the critical yield strain is defined as $\gamma_y(\phi) \approx \sigma_y(\phi) / G'(\phi)$, the adimensional yield strain obeys a similar law:

$$\frac{\gamma_y(\phi)}{\gamma_0} = \sqrt{(1-\phi)\left(1-\phi/\phi_m\right)^{2.5\phi}} \qquad (5)$$

We see that the scaling law captures reasonably well the experimental trends, with a least square fitting $R^2 = 0.92$. Deviations from the theoretical predictions can originate from clustering of the fillers.

From these observations, we infer that measuring the linear properties of particle-filled lipid gel networks with granular fillers enable us to estimate nonlinear properties such as the yield stress and strain, even when these systems depart from ideality. It is noteworthy that the impact of

granular fillers on lipid gels differs from colloidal fillers, where both the elastic moduli and yield stress are expected to obey roughly the same scaling with volume fraction. Future studies concern the investigation of the mechanics of starch fillers endowed with attractive interactions and embedded in a similar lipid gel network.

Overall, our findings are in good qualitative agreement with those reported in ideal isotropic suspensions of monodispersed rigid spherical noncolloidal particles embedded in emulsions, bentonite and Carbopol gel suspensions.

4. CONCLUSIONS

We have investigated experimentally the mechanical contribution of rigid granular starch particles to lipid crystal networks. We focused on the influence of volume fraction on the elastic modulus, yield stress and yield strain of the suspensions. As the filler volume fraction increases, the starch-filled lipid gels gradually stiffen and become brittle, reminiscent of hard passive fillers. The dimensionless elastic modulus $G'(\phi) / G_0'$ depends only on starch volume fraction ϕ, which obeys a Krieger-Dougherty law $(1 - \phi/\phi_m)^{-2.5\,\phi_m}$ with $\phi_m = 0.53$. The yield stress/concentration are related to the elastic modulus/concentration relationship through a simple scaling law $\sigma(\phi)/\sigma_y(0) = \sqrt{(1-\phi)G'(\phi)/G_0'}$, proposed for more ideal soft suspensions filled with hard monodisperse spheres. We anticipate that similar relationships will hold for granular passive fillers integrated in concentrated-to-dense food suspensions.

ASSOCIATED CONTENT

Additional confocal micrographs, strain sweep and stress growth curves are included in the Supporting Information, which is available free of charge.

AUTHOR INFORMATION

Corresponding Authors:

*E-mail: braulio.rodriguez@unilever.com, krassimir.velikov@unilever.com

Notes

The authors declare no competing financial interest.

ACKNOWLEDGMENTS

The authors thank Ziya Lan for collecting part of the experimental data presented in this work. The authors also thank Daniel Bonn at the University of Amsterdam, for insightful discussions while preparing this article. This project has received funding from the European Union's Horizon 2020 research and innovation programme under the Marie Sklodowska-Curie grant agreement No. 798917.

REFERENCES

Behringer, R. P., & Chakraborty, B. (2018). The physics of jamming for granular materials: a review. *Reports on Progress in Physics*, *82*(1), 012601

Blanco, E., Hodgson, D. J., Hermes, M., Besseling, R., Hunter, G. L., Chaikin, P. M., ... & Poon, W. C. (2019). Conching chocolate is a prototypical transition from frictionally jammed solid to flowable suspension with maximal solid content. *Proceedings of the National Academy of Sciences*, *116*(21), 10303-10308

Dinkgreve, M., Paredes, J., Denn, M. M., & Bonn, D. (2016). On different ways of measuring "the" yield stress. *Journal of non-Newtonian fluid mechanics*, *238*, 233-241

Frith, W. J., & Lips, A. (1995). The rheology of concentrated suspensions of deformable particles. *Advances in colloid and interface science*, *61*, 161-189

Genovese, D. B. (2012). Shear rheology of hard-sphere, dispersed, and aggregated suspensions, and filler-matrix composites. *Advances in colloid and interface science*, *171*, 1-16

Hashin, Z., & Shtrikman, S. (1963). A variational approach to the theory of the elastic behaviour of multiphase materials. *Journal of the Mechanics and Physics of Solids*, *11*(2), 127-140.

Heinrich, G., Klüppel, M., & Vilgis, T. A. (2002). Reinforcement of elastomers. *Current opinion in solid state and materials science*, *6*(3), 195-203

Mahaut, F., Chateau, X., Coussot, P., & Ovarlez, G. (2008). Yield stress and elastic modulus of suspensions of noncolloidal particles in yield stress fluids. *Journal of Rheology*, *52*(1), 287-313.

Mermet-Guyennet, M., Dinkgreve, M., Habibi, M., Martzel, N., Sprik, R., Denn, M., & Bonn, D. (2017). Dependence of nonlinear elasticity on filler size in composite polymer systems. *Rheologica Acta*, *56*(6), 583-589

Mitarai, N., & Nori, F. (2006). Wet granular materials. *Advances in Physics*, *55*(1-2), 1-45

Poon, W. C., Weeks, E. R., & Royall, C. P. (2012). On measuring colloidal volume fractions. *Soft Matter*, *8*(1), 21-30

Richards, J. A., Guy, B. M., Blanco, E., Hermes, M., Poy, G., & Poon, W. C. (2020). The role of friction in the yielding of adhesive non-Brownian suspensions. *Journal of Rheology*, *64*(2), 405-412

Schroeter, J., & Hobelsberger, M. (1992). On the mechanical properties of native starch granules. *Starch-Stärke*, *44*(7), 247-252

Shewan, H. M., Deshmukh, O. S., Chen, G., Rodrigues, S., Selway, N., & Stokes, J. R. (2021). Interpreting rheological behaviour of sugar-fat mixtures as a function of solids phase volume. *Journal of Food Engineering*, *297*, 110474

Wijmans, C. (1998). Brownian dynamics simulations of filled particle gels. *Journal of the Chemical Society, Faraday Transactions*, *94*(1), 129-137

Zhou, J. Z., Uhlherr, P. H., & Luo, F. T. (1995). Yield stress and maximum packing fraction of concentrated suspensions. *Rheologica acta*, *34*(6), 544-561.

Scholten, E. (2017). Composite foods: from structure to sensory perception. *Food & function*, *8*(2), 481-497.